Natural Hazards
https://doi.org/10.1007/s11069-018-3557-8

ORIGINAL PAPER

Land use change increases flood hazard: a multi-modelling approach to assess change in flood characteristics driven by socio-economic land use change scenarios

Jean Hounkpè[1,2] · Bernd Diekkrüger[3] · Abel A. Afouda[1,2] · Luc Olivier Crepin Sintondji[2]

Received: 12 March 2018 / Accepted: 17 December 2018

Abstract
We analysed in the work how change in land use/land cover influences on flood characteristics (frequency and magnitude) using a model inter-comparison approach, statistical methods and two land use scenarios (land use scenario A and land use scenario B) for three time horizons. The derived land use maps from these scenarios were considered as forcing inputs to two physically based hydrological models (SWAT and WaSiM). The generalized Pareto distribution combined with the Poisson distribution was used to compute flood frequency and magnitude. Under land use scenario A, croplands increase at the annual rate of 0.7% while under land use scenario B, it increases by 1.13% between 2003 and 2029. The expansion of croplands indubitably enhances flood risks. Although there was a general agreement about the sense of the variation, the magnitude of change in flood characteristics was highly influenced by the model type. The rate of increase in flood quantiles simulated from SWAT (0.36–1.3% for 10-year flood) was smaller than the corresponding magnitude of changes simulated from WaSiM (2.6–7.0% for 10-year flood) whatever the scenarios. The expansion of agricultural and pasture lands at the yearly rate of 0.7% under land use scenario A (respectively, 1.13% under land use scenario B) leads to an increase of 3.6% (respectively, 5.4%) in 10-year flood by considering WaSiM. This study is among the first of its kind to establish a strong statistical relation between flood severity/frequency and agricultural land expansion and natural vegetation reduction. The results of this study are relevant and useful to the scientific research community as well as the decision makers for framing appropriate policy decisions towards the management of extreme events and the land use planning/management in future in the region.

Keywords Flood events · Multi-modelling · Statistical analysis · Zou catchment · West Africa

✉ Jean Hounkpè
jeanhounkpe@gmail.com

Extended author information available on the last page of the article

Published online: 05 January 2019

1 Introduction

Global changes including the change in land distribution and climate could result in high modification of the hydrological processes and water cycle. Changes in Land Use and Land Cover (LULC) are currently observed and will persist at high rates in Benin, West Africa, mainly because of the increase in population (Menz et al. 2010). For water resources evaluation and management, it is important to quantify beside climate change (Mendizabal et al. 2014) to which extent LULC change impacts the basin hydrology and mainly on the flood regime. Previous studies help to understand how change in LULC impacts on hydrology including flood regime in different climate conditions (see Table 1). Several methods to evaluate the hydrological impacts of environmental changes have been developed (Li et al. 2009) including the hydrological modelling. Key papers on this approach are presented in Table 1.

Most of the studies done by applying rainfall-runoff modelling are based on single hydrological model (see Table 1). Nevertheless, to deal with uncertainties in prediction, model inter-comparison and multi-model ensembles could be an efficient tool. For instance, Bormann et al. (2009), Huisman et al. (2009) and Viney et al. (2009) during the LUCHEM project applied multi-models ensemble techniques to evaluate how change in LULC influences on the hydrological processes of the Dill watershed located in Federal Republic of Germany. They found substantial differences in model evaluation criteria (for calibration and validation) but concordant results about the variation in mean yearly streamflow and high streamflow from the prediction of the scenarios. Cornelissen et al. (2013) used four hydrological models combined with land use scenarios in Térou Catchment and conclude that LULC change substantially influences on streamflow. Nevertheless, the results of the models during both calibration and validation, and scenarios analysis were not consistent questioning the reliability of other studies based on single hydrological modelling. Similar results were found in other model inter-comparison studies in hydrology (Diekkrüger et al. 1995; Refsgaard and Knudsen 1996). Besides, none of these multi-modelling studies focuses on flood frequency analysis of the output discharge obtained through the scenarios analysis despite the recurrence of flood worldwide (Hounkpè 2016) and its disastrous impacts on human and properties.

For land use change impact assessment, mainly distributed models (De Roo et al. 2001, 2003; Thanapakpawin et al. 2006; Yira et al. 2016) and semi-distributed models (Crooks and Davies 2001; Kharel et al. 2016) are preferred given that they provide greater details about the hydrological processes (Beven 2012). Bronstert et al. (2002) emphasized that while analysing of the LULC impacts, it is essential to consider process-based hydrological model. Considering these recommendations, WaSiM (Schulla 2012) and SWAT (Arnold et al. 1998) hydrological models that were successfully used in hydrological impact studies and flood simulation purpose (Cullmann et al. 2006; Kunstmann et al. 2006; Herbst et al. 2009; Seidou et al. 2012a, b; Kharel et al. 2016) were chosen.

It is important to know what will be the change in flood characteristics for a given peak discharge after change in a particular land use type. This knowledge is of significant interest for water resources management including flood management (Guo et al. 2008), and it can help to select appropriate flood protection measures. Often, studies concentrate on climate change with a focus on 2050–2100, but land use change is currently happening at a much faster rate and the impact of LULC on flood hazard is often ignored. This study aims to determine through a combination of a multi-modelling approach and statistical analysis the extent to which LULC changes influence the flood frequency and severity of a

Table 1 Selected relevant studies on LULC change impact on hydrology

	Study	Considered data/model	Catchment/climate/catchment area	Important results		
				Assess the change in LULC	Evaluate hydrological model performance and suitability considering peak discharge	- Evaluate LULC change influence on discharge - Perform model intercomparison and multi-modelling - Explicitly relate change in flood characteristics to change in land use through flood frequency analysis.
0	This study	SRTM 90-m, Landsat maps, gauge data (climate, discharge)/ WaSiM, SWAT	Zou catchment, Benin/tropical humid/7035 km^2	An increase in croplands at annual rate of 0.7% under LUA and 1.13% between 2003 and 2029	Very good to unsatisfactory model performance depending on thresholds and performance criteria	- An increase in croplands or decrease in natural vegetation enhance flood characteristics (frequency and magnitude) - Both models agreed on the change direction of flood characteristics (mean ensemble members) with considerable differences in the magnitude of model outputs for the different scenarios - Very strong linear relation was established between flood characteristics and changes in each land use type

Table 1 (continued)

1	Crooks and Davies (2001)	Observed land use maps, gauge data/CLASSIC	Thames River/ Britain/tempered climate/9948km2	Land use modification for thirty years with a time step of 5 years	Good model performance was obtained	- The influences of the modification in land use distribution on flood recurrence have been very small during the study period (1961–1990) - N/A - N/A
2	De Roo et al. (2001)	Guage data, Corine land cover and Landsat data, DEM 75 m and 1 km/ LISFLOOD	Meuse and Oder Catchment, transnational European river basins/tempered climate/32,457 and 59,162 km^2	Slight change in land use of Oder (Meuse) catchment between 1975 and 1992	Reasonably good model performance	- 0.20% increase in high streamflow and 4.06% increase in the total volume of flood water resulting from the difference in land use maps - N/A - N/A
3	Costa et al. (2003)	Gridded global CRU climate dataset, gauge data/no model used	Tocantins River/tropical climate/175,360 km^2	A substantial expansion of cultivated area from 30% in 1960 to 49% in 1995 (cropland and pastures)	N/A	- Between these two periods, an increase of 24% of the annual mean discharge and 28% of high-flow season discharge were observed - N/A - N/A
4	De Roo et al. (2003)	Guage data, Corine land cover and Landsat data 100 m, DEM 1 km/LISFLOOD	Oder Catchment, transnational European river basins/tempered climate/59,162 km^2	Increase in forests, urban areas and decreased in arable land between 1780 and 2001	High coefficient of correlation between measured and model output discharges at most of the gauging stations	- Peak discharges increased due to urban growth in the Oder - N/A - N/A

Table 1 (continued)

5	Thanapakpawin et al. (2006)	DEM 150 m, FAO Soil Map, gauge data, land use data observed and scenario/DHSVM	Mae Chaem Catchment, Thailand/tropical climate/3853 km^2	Increase in cropland from 10.4% to 19.9%	Model performances were not consistent across subbasin during both calibration and validation	- Increase in agricultural land increases the dry-season flow as well as the annual and wet-season flow - N/A - N/A
6	Huisman et al. (2009)	DEM 25 m, soil digital data 25 m, multi-temporal set of Landsat images/10 Models	Dill catchment, Germany/tempered climate/693 km^2	Agricultural land raises to 33% while pasture area decreased by 11% and forest by 22%	Substantial differences in the performances of models were observed	- Increase in average yearly streamflow induced by the increase in field size predicted by all models - Almost an increase in the average yearly and high streamflow simulated by the models considering the different scenarios - N/A
7	Cornelissen et al. (2013)	Observed data, Landsat images, SRTM 90 m/ GR4 J, WaSiM, SWAT, UHP-HRU	Térou watershed, Benin/sub-humid region/2344 km^2	N/A	Good performance criteria obtained for all models	- Expansion of croplands leads to an increase in discharge - No consistency found in models results from scenario analysis - N/A
8	Jothityangkoon et al. (2013)	Observed data, Landsat images, Soil data/ catchment flood routing model	Ping river/tropical climate/26,38 6 km^2	Deforestation by 10%, 20%, 30%	N/A	- Forest reduction by 10%, 20%, 30% can result in an increase of 3.1%, 6.2%, 9.2%, respectively, of Probable Maximal Flood - N/A - N/A

Table 1 (continued)

9	Kharel et al. (2016)	Observed gauge data, 4 land use scenarios alternatives based on the market and policy conditions, 15 general circulation models (GCMs)/SWAT	Devils Lake basin/ temperate climate/9800 km^2	LULC scenarios formulated considering projected crop prices and flooding mitigation policy	Good model performance	- The surface runoff varies significantly (−6.5 : 9.9%) due to change in LULC; Incentivized grass and alfalfa scenarios moderated the influences on hydrological processes - N/A - N/A
10	Yira et al. (2016)	SRTM 90 m, Landsat and RapidEye-derived maps, observed gauge data, soil hydraulic properties measurement on the field/WaSiM	Dano catchment, Burkina Faso/tropical sub-humid/195 km^2	Reduction in savannah at yearly rate of 2% since 1990	Model performances using soil moisture, discharge and groundwater level were acceptable	- High correlation between LULC and streamflow was found, LULC change leads to an increase in discharge up to 5% - N/A -Changes in water balance components were explicitly related to change in LULC

N/A representing 'not applicable' indicates that the study did not account for the mentioned components

tropical, predominantly agricultural catchment. This paper has three specific objectives: (1) to assess LULC change based on socio-economic scenarios; (2) to evaluate hydrological model suitability and performance in simulating high discharge; and (3) to assess LULC change impact on flood regime using multi-modelling approach and explicitly relate change in flood characteristics to change in land use through flood frequency analysis (FFA).

2 Study site and materials

The study area (Zou catchment) is part of the Ouémé catchment located mostly in Benin Republic with an area of 7035 km^2 (Fig. 1). Considering the different rainfall regimes, the Ouémé basin can be split into three climatic zones: the north with a unimodal rainfall regime, the south with a bimodal rainfall regime and the middle situated in a transition rainfall area between the two previous regimes. The Zou catchment is situated in this transition area. Rains mostly originate from the Guinean coast. The Zou catchment records

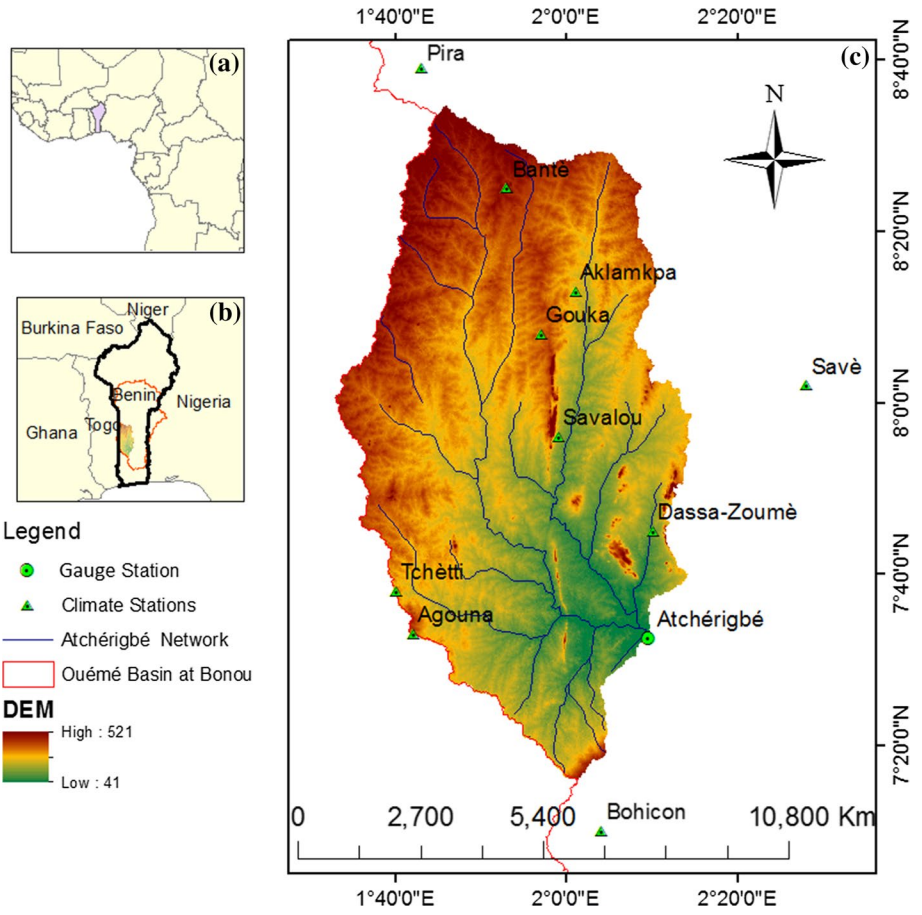

Fig. 1 Overview of the Ouémé and Zou (at Atchérigbé gauge) basins: (**a**) Benin Republic in Africa; (**b**) position of Zou and Ouémé basins in Benin and (**c**) Zou basin, its relief and the climate stations

annual minimal and maximal temperatures of 23–33 °C and has an average yearly precipitation of 1162 mm for 1991–1998 and 1219 mm for 1999–2010. The main land use types in the catchment are savannah, croplands and pastures, forest islands, woodlands, gallery forest.

Geographic, climatic and discharge data were collected. The geographic data considered are the digital elevation model (DEM) SRTM at 90 m resolution (Jarvis et al. 2008), land use data obtained from RIVERTWIN project (RIVERTWIN 2007) at 250 m resolution and soil data (Bossa et al. 2014). The dominant soil types are Albic Plinthosol (22%), Mollic Gleysol (20%), Ferric Luvisol (20%) and Haplic Arenosols (15%).

The meteorological data used are rainfall, temperature, wind speed, relative humidity, global radiation and/or sunshine duration obtained from the Benin national directorate of meteorology for the 1991–2010. In addition, discharge data were received from Benin national water directorate (1991–2010).

3 Methods

3.1 Land use and land use change scenario

A land use/land cover (LULC) map was built within the RIVERTWIN project (RIVERTWIN 2007) at the scale of 1/200.000 using Landsat images in 2003 (Igué et al. 2006). After image treatment, imaged maps were established and interpretation keys were defined. For efficacy reasons, the interpretation was carried out at the scale of 1/50.000 in order to get maximum information and more than 650 observation points ground data were available. Finally, 17 land use/cover classes were defined. The subsequent accuracy check shows that the overall interpretation accuracy is high (87%) (Igué et al. 2006; RIVERTWIN 2007). This map of 2003 was considered as the baseline map. The 2003 LULC map was preferred to the classification of new LULC maps to avoid uncertainties due to different classification methods. In fact, the 2003 map as well as the future land use projection maps was built by experts in the field during the RIVERTWIN (2007) project.

In the Ouémé basin, the major driver for LULC modification is the increase in the number of inhabitants and the accompanying expansion of cropland, settlement and roads at the detriment of natural vegetation. Two socio-economic scenarios were established denoted as LUA and LUB herein (RIVERTWIN 2007). Land use scenario A (LUA) is characterized by a relatively strong economic development, moderated cities grow, promotion of irrigated agriculture and an annual population growth of 3.2%. Land use scenario B (LUB) is characterized by a weak economic development, a weak land use planning and expansion of rainfed agriculture, and a 3.5% annual increase in population (Götzinger 2007). Based on the distance to the roads and existing villages, new settlements and agricultural areas have been generated leading to new land use distribution.

3.2 Hydrological modelling

3.2.1 Model description and model structure inter-comparison

For the hydrological modelling, two models were selected: SWAT (Arnold et al. 1998) and WaSiM (Schulla 2012). These models are largely used to evaluate water balance, global change impact on hydrology and water resources in West Africa (D'Orgeval 2006; Wagner

2008; Kasei 2009; Bossa 2012). Besides, WaSiM model is designed for flood simulation—single event as well as continuous simulation of floods—(Schulla 2012) and was successfully applied by many authors for flood modelling purpose (Jasper et al. 2002; Cullmann et al. 2006; Kunstmann et al. 2006; Herbst et al. 2009; Crochet 2012). SWAT has been used by some authors for flood modelling (Seidou et al. 2012a, b; Kharel et al. 2016).

SWAT is a semi-distributed model while WaSiM is a distributed model (Table 2). They are both mainly physically based and time continuous watershed models. SWAT divides the basin into subbasins. The subbasins are further split into Hydrological Response Units (HRU) based on a DEM, but WaSiM discretizes the catchment into grids cells. Like the grid cells, the HRUs are homogeneous concerning soil, slope and vegetation. Both models split the soil into several numerical layers, but Richards equation (Richards 1931) is applied to soil module in WaSiM while a tipping bucket approach is considered in SWAT. The models differ also considering the interflow computation. In WaSiM, the interflow is computed using the Darcy´s law depending on hydraulic conductivity, soil moisture and slope while in SWAT it is calculated based on the kinematic storage model. Both models use the linear storage approach for describing the baseflow. For SWAT, direct runoff component is derived from a modified SCS curve number method (Chow et al. 1988) where surface flow is computed as a function of land use, soil type and previous moisture condition. Peak runoffs are generated using a modified rational formula (Chow et al. 1988). In WaSiM, runoff is computed either by infiltration excess (rainfall intensity is greater than infiltration rate, Hortonian runoff) or by saturation excess. The infiltration is derived from Richards equation in WaSiM, whereas the SCS curve number is considered in SWAT. SWAT was run with 2076 HRUs within 49 subbasins, and WaSiM was run at 0.25 km^2 resolutions.

3.2.2 Soil and land use parameterization in SWAT and WaSiM

For each land use type, WaSiM requires fifteen parameters. Five parameters are constant in time (the root density distribution, the relative soil moisture value for beginning of water stress, the minimum relative reduction factor of real transpiration when water content reaches saturation, the hydraulic head for beginning dryness stress and the specific thickness of the water layer on the leaves). Other remaining ten parameters vary in function of time (plant development stages, albedo, leaf surface resistance, interception surface resistance, soil surface resistance (for evaporation), leaf area index, roughness length, vegetation covered fraction, root depth, shift in temporal vegetation development per metre elevation).

Table 2 Hydrological processes computation in WaSiM and SWAT

Hydrological aspect	WaSiM (Schulla 2012)	SWAT (Arnold et al. 1998)
Model type	Distributed	Semi-distributed
Spatial unit	Hydrological Response Units (HRU), 2076 HRUs	Grid cells with a size of 0.5 km
Soil module	Richards equation	Tipping bucket approach
Interflow module	Darcy´s law	Kinematic storage model
Baseflow module	Linear storage approach	
Direct runoff module	Infiltration excess or saturation excess	SCS curve number
Infiltration module	Richards equation	SCS curve number

The values attributed to these parameters were obtained from the literature (Kasei 2009; Cornelissen et al. 2013).

For each soil type in WaSiM, nine parameters must be provided (saturated water content, residual water content, saturated hydraulic conductivity (Ks), the empirical van Genuchten parameters α and n, number of horizons per soil unit, number of numerical layers per soil unit, thickness of soil layers and recession of Ks with depth). The van Genuchten parameters are computed by applying a pedotransfer function. The saturated water content (Ks) and the recession of Ks with depth were calibrated.

In SWAT, soil is characterized by its hydrologic group based on the infiltration characteristics of the soil, namely, soil texture, effective soil depth and shrink–swell potential, soil depth, organic carbon content, soil texture distribution, bulk density, available water capacity and saturated hydraulic conductivity. The hydraulic properties were obtained from field work (Sintondji 2005; Bossa 2012) and using a pretransfer function (Rohstoffe and Hannover 1993). The initial land use types have been adjusted to the predefined SWAT land use types for which different parameters were defined by default.

3.2.3 Model calibration and validation

Model calibration consists of adjusting the model parameters values for matching the simulation and observation data. Given that process-based models were considered in this work, a limited number of parameters were calibrated (see Table 7). Hundreds of simulations were performed automatically using the Latin Hypercube method (McKay et al. 2000) for generating the set of parameters used, and the different objective functions (see below) were computed. The partial correlation coefficient and its significance were considered to assess the relationship between the performance criteria and the corresponding parameters. In addition, graphical analysis of the scatter plot of the objective functions and the calibrated parameters permit the identification of the optimized set of parameters.

A time period of 20 years was used for this simulation (1991–2010) at a time step of one day. The calibration was done for 2005–2009 and the validation for 1991–1998 using the land use of 2003. Performing the calibration and the validation with the same land use map of 2003 implies that the land use does not vary during this period. This assumption (not necessarily verified) could impact negatively on the simulation results mainly during the validation. The objective functions used are the Kling and Gupta Efficiency (KGE) (Gupta et al. 2009) and the absolute percentage bias (APB) considering different discharge thresholds during calibration and validation. KGE and APB were evaluated considering the ranges defined by Moriasi et al. (2007) (for KGE: very good: 0.75–1.0, good: 0.65–0.75, satisfactory: 0.5–0.65, unsatisfactory: < 0.5; for APB: very good: $< |10|$, good: $|10|–|15|$, satisfactory: $|15|–|25|$, unsatisfactory: $\geq |25|$).

3.3 Modelling the LULC change impact on flood characteristics

3.3.1 Land use change scenario implementation

LULC change scenarios consist of natural vegetation conversion into agriculture lands and pasture for the Zou catchment at Atchérigbé station. In the Ouémé basin, the major driver for land use change is population growth (Götzinger 2007). Together with stakeholders, two socio-economic scenarios were set up during the RIVERTWIN project (RIVERTWIN 2007). Land use scenario A is characterized by a stronger economic development, controlled

urbanization, the implementation of two large-scale irrigation schemes and 3.2% population growth per year while land use scenario B is characterized by a weak national economy, uncontrolled settlement and farmland development and a 3.5% population growth per year (Götzinger 2007). These scenarios are also used for national planning by the administration of Benin. For each scenario, the population growth has been translated into a specific demand for settlements and agricultural area according to the development of the national framework. According to the proximity to roads and existing villages, new settlements and agricultural areas have been created leading to new land use distribution. Therefore, large areas of natural vegetation were converted to croplands and pasture land (Bossa et al. 2014).

Three time slices have been considered for each land use scenario: 2015–2019; 2020–2024; and 2025–2029. A combination of the two scenarios with the three time horizons leads to six different land use distributions. For example, LU2017A corresponds to the land use scenario A for the time window 2015–2019 (Table 3). Similarly, LU2027B corresponds to the land use scenario B for the time horizon 2025–2029 and so on. All different land use distributions were used for simulating discharge using the same climate data of 1991–2010 to be able to derive the exclusive influence of land use change on the model outputs.

After the calibration and validation of the hydrological model using the 2003 land use, the following step was the implementation of land use change scenarios. This implies running the two models with the parameters obtained from the current land use condition but with different land use classes and spatial distributions. The same parameters (10 best sets of parameters) are used for the present and future (scenario) conditions for reducing model parameter uncertainties. As stated by Huisman et al. (2009), a key factor while assessing the LULC change impact on water resources is to consider the differences in evaporation and transpiration of different land use types. For that purpose, the same method for the computation of ETP was used for both models, namely, the Penman–Monteith method. On the other hand, soil properties (hydraulic conductivity, storage capacity) are strongly influenced by the vegetation types so change in LULC types will influence on soil properties, especially in WaSiM. In SWAT, this change is covered by the SCS curve number which depends on local land use and soil type.

3.3.2 Flood characteristics calculation

Where long-term data are available, discharge data can be fitted to a statistical distribution considering data sampling method such as annual maximum series or peaks over threshold (POT) to estimate flood characteristics (frequency and magnitude) (Beven 2012). Due to the data length (1991–2010), the peak over threshold approach was adopted in this work and the generalized Pareto distribution (GPD) chosen. The GPD cumulative distribution function is as follows:

$$\begin{cases} F(Y \le y|\sigma,\kappa) = 1 - \left[1 + \kappa.\left(\frac{y}{\sigma}\right)\right]^{\frac{-1}{\kappa}}; \quad \kappa \neq 0 \text{and} \quad 1 + \kappa\left(\frac{x}{\sigma}\right) > 0 \\ F(Y \le y|\sigma,\kappa) = 1 - \exp\left(-\frac{y}{\sigma}\right) \qquad \kappa = 0 \qquad \sigma > 0 \end{cases} \tag{1}$$

Table 3 Different land use scenarios with the corresponding time horizons

Time horizons and land use scenarios	2015–2019	2020–2024	2025–2029
LUA	LU2017A	LU2022A	LU2027A
LUB	LU2017B	LU2022B	LU2027B

κ (respectively, σ) is the shape (respectively, scale) parameter.

The occurrence of events is assumed to be a Poisson process. Let N be the number of time an event has occurred per year and λ the average of occurrence per year, the number n of events that can occur considering any given year can be considered as Poisson variate (Beguería 2005):

$$P(N = n|\lambda) = e^{-\lambda} * \frac{\lambda^n}{n!}, \quad n = 1, 2, \ldots \tag{2}$$

The Poisson assumption involves the independence of λ. The dispersion index DI which is the proportion between the variance and the mean is expected to equate the unit for a Poisson distribution (Beguería 2005). This is an important property which can help to find the threshold x_0 from which the selected POT data follow the Poisson process. Nearly independent peaks were selected using the criteria described by Willems (2014). The independency between two consecutive peaks is accepted if the recession constant k is smaller than the time between the aforementioned two peaks. Additionally, the peak must be greater or equal to the selected threshold. For each threshold, the corresponding dispersion index (DI) is computed.

In this study, two flood characteristics were investigated: changes in flood magnitude and flood frequency. A comparison between quantiles on the one hand and return periods on the other hand will give an indication on how future land cover will impact the flood regime.

4 Results

4.1 Land use change scenarios

Agriculture land increases from 45% in 2003 to 48% for scenario A (to 57% for scenario B) in 2029 (Table 4). Pasture increases from 9% in 2003 to 24% for scenario A (to 26% for scenario B) in 2029 at the detriment of natural vegetation such as range brush and grasses, forests (deciduous and evergreen). The range brush and grasses (abbreviations RNGB and RNGE, see Table 4) had decreased from 24% in 2003 to 14% for scenario A (to 9% for scenario B) in 2029. For the same time span, forests (abbreviations FRSD, FRST, FRSE, see Table 2) had decreased from 20% to 14% for scenario A (to 9% for scenario B). Wetland forests (0.1%) and agglomeration (0.6%) were relatively unchanged for both scenarios. Overall, under land use scenario A (LUA), cropland and pasture increase at the annual rate of 0.7%, but under land use scenario B (LUB), it increases by 1.13% between 2003 and 2029. Conversely, the natural vegetation decreases at annual rate of 0.7% under LUA compared to a decrease of 1.13% under LUB. The increases in cropland areas were shown by many authors (Orekan 2007; Yira et al. 2016) in the region confirming the validity of the scenarios applied in this study.

4.2 Hydrological modelling

Given that the focus of this work was on peak discharge at daily time steps, the calibration was done using the threshold of 120 m^3/s (1.5 mm/d) (Hounkpè 2016). Different sets of parameters lead to acceptable performance criteria implying the equifinality concept as defined by Beven and Freer (2001). The calibrated parameters and their ranges for

Table 4 Repartition (in percentage) of the LULC types in each scenario with the corresponding time horizon and the slope corresponding to the linear regression over time

% LULC	LU2003 (2003)	LU2017A (2015–2019)	LU2022A (2020–2024)	LU2027A (2025–2029)	Slope (2003–2029)	LU2017B (2015–2019)	LU2022B (2020–2024)	LU2027B (2025–2029)	Slope (2003–2029)
FRSD	4.1	3.6	3.5	3.3	−0.03	2.9	2.5	2.0	−0.09
FRST	12.3	9.6	9.0	8.4	−0.16	7.6	6.2	4.6	−0.32
RNGB	23.6	16.4	14.6	13.2	−0.44	13.8	11.0	8.2	−0.65
AGRL	45.4	48.0	48.0	47.7	0.10	52.2	54.0	55.8	0.44
FRSE	4.0	2.4	2.4	2.4	−0.07	2.4	2.4	2.4	−0.07
RNGE	0.5	0.5	0.5	0.5	0.00	0.5	0.5	0.5	0.00
URML	0.6	0.6	0.6	0.6	0.00	0.6	0.6	0.6	0.00
WETF	0.1	0.1	0.1	0.1	0.00	0.1	0.1	0.1	0.00
PAST	9.4	18.7	21.3	23.8	0.60	19.8	22.8	25.7	0.69

The different land use types are forest deciduous (FRSD), forest mixed (FRST), range bush (RNGB), agriculture (AGRL), forest evergreen (FRSE), range grasses (RNGE), urban area (URML), wetlands forest (WETF) and pasture (PAST)

the ten best simulations based on the Latin Hypercube sampling are shown in Table 7 in "Appendix".

During calibration and validation using a threshold of 120 m^3/s (1.5 mm/d), WaSiM performances were satisfactory according to both KGE (between 0.5 and 0.6) and APB (between 0.32 and 19.44). At the same threshold, SWAT performances were satisfactory according to APB (between 6.26 and 15.42) but unsatisfactory according to KGE (between 0.35 and 0.4) (see Table 5). At thresholds lower than 1.5 mm/d, model performances were satisfactory, good or very good and the highest model performances correspond to the lowest thresholds. The water balance components simulated were in the range of what is regionally observed (Kasei 2009; Cornelissen et al. 2013) (Table 6). The simulated and measured discharges during calibration and validation are observed in Fig. 2. It can be concluded that both models simulated acceptably the high and lower discharges.

4.3 LULC change impact on flood characteristics

4.3.1 The threshold selection and Poisson assumption

For the different thresholds selected, the corresponding dispersion index (DI) is computed. For both SWAT and WaSiM models, the condition of DI = 1 was satisfied for many thresholds (Fig. 3). Given that we had 20 years data, the choice of the threshold was done in a way that the average occurrence per year is greater or equal to 1.5 to achieve at least 30 data points selected for each simulation. It was found that the condition of DI = 1 was nearly satisfied around the threshold of 130 m^3/s for WaSiM. The corresponding average rate of occurrence per year (Lambda) is 2.43. Therefore, given that 20 years of discharge data were used in this analysis, the approximate POT data size will be 2.43*20 = 49 which is sufficient to perform statistical analysis. For SWAT, the condition of DI = 1 is nearly satisfied around the threshold of 140 m^3/s and the corresponding Lambda is 1.97. This implies that the average number of data above the selected threshold is 1.97*20 = 39 which is an acceptable data sample required in statistical analysis. The distribution of DI for overall 70 samples derived from WaSiM and SWAT outputs (for the scenarios) was between 0.8 and 1.2 (1 ± 0.2) which is an acceptable measure in achieving a fundamental property of the Poisson process distribution. In addition, we applied the Mann–Kendall trend to test the stationarity of each dataset. This test found no trend in the data.

After applying the criteria of Willems (2014) for the selection of independent peaks in such a way that the dispersion indexes were nearly equal to one with each data size greater or equal to 30 (the minimum sample required for obtaining accurate results from a statistical distribution) and verifying the stationarity of the selected data, we can proceed to flood frequency analysis based on GPD for flood quantile estimation and the associated Poisson distribution for the frequency analysis.

4.3.2 Relating change in flood quantiles to change in LULC

4.3.2.1 Change in flood quantiles Due to the difference in model concepts (Beven 2012) and for reducing errors due to input data and uncertainties due to the difference in the two models' structure, the analysis was concentrated on change in quantiles which is common in scenario analysis (Arnell 1999; IPCC 2001; Huisman et al. 2009; Vaze and Teng 2011; Teng et al. 2012) rather than absolute values. Figure 4 shows the percentage change in quantiles (mean over the ten behavioural solutions) computed relatively to the baseline by

Table 5 Performance criteria of WaSiM and SWAT models during calibration (2005–2009) and validation (1991–1998) with a threshold of 120 m^3/s (1.5 mm/day) based on 10 behavioural simulations

	Calibration						Validation					
	WaSiM			SWAT			WaSiM			SWAT		
	Min	Mean	Max	Min	Mean	Max	Min	Mean	Max	Min	Mean	Max
KGE	0.50	0.54	0.60	0.36	0.37	0.40	0.50	0.52	0.54	0.35	0.37	0.39
	Satisfactory			Unsatisfactory			Satisfactory			Unsatisfactory		
APB	0.32	3.39	8.21	10.23	12.65	15.42	9.85	16.04	19.44	6.26	8.46	9.98
	Very good			Good			Good/satisfactory			Very good		

Table 6 Water balance components as simulated by WaSiM and SWAT models during calibration (2005–2009) and validation (1991–1998) with a threshold of 120 m^3/s (1.5 mm/day) based on 10 behavioural simulations

	Calibration						Validation					
	WaSiM			SWAT			WaSiM			SWAT		
	Min	Mean	Max	Min	Mean	Max	Min	Mean	Max	Min	Mean	Max
CoefRun (%)	15.24	16.14	18.00	16.04	16.25	16.69	11.46	12.24	13.68	12.26	12.51	13.03
CoefETR (%)	82.13	83.92	84.86	66.60	66.83	67.09	85.84	87.10	87.81	70.65	70.89	71.14
Rainfall (mm/day)	1179	1179	1179	1193	1193	1193	1158	1158	1158	1166	1166	1166
Total Run-off (mm/day)	180	190	212	191	194	199	133	142	158	143	146	152
Interflow (mm/day)	139	151	164	2	5	15	102	110	122	2	4	12
Overland (mm/day)	13	17	21	125	133	140	10	12	16	101	107	114
Baseflow (mm/day)	12	22	35	43	56	64	10	20	30	25	35	41
ETR (mm/day)	968	989	1000	795	797	801	994	1008	1017	824	827	830
ETP (mm/day)	2239	2306	2344	1509	1509	1509	2248	2317	2357	1514	1514	1514
Storage (mm/day)	−5	−1	2	15	17	18	5	8	9	14	15	16
SHL_AQ_R (mm/day)	–	–	–	177	185	190	–	–	–	170	179	183

ETR corresponds to the real evapotranspiration; SHL_AQ_R is the shallow aquifer recharge and APB is the absolute percentage bias; ETP is the potential evapotranspiration. CoefRun (CoefETR) is the percentage of the mean annual discharge (ETR, respectively) to the mean annual rainfall

SWAT (Fig. 4a) and WaSiM (Fig. 4b) for different return periods. Both models agreed on the change direction for all return periods, strengthening our confidence in the analysed scenarios. Whatever the scenario considered an increase in flood quantiles was simulated by all models. Nevertheless, the magnitude of changes simulated from SWAT output was significantly smaller than the corresponding magnitude of changes simulated from WaSiM output. Both models successfully reproduced the difference in the two scenarios (LUA and LUB) into their outputs. The increase in flood quantile under LUA is lower than the increase in flood quantile under LUB. In fact, the expansion of agricultural and pasture lands at the yearly rate of 0.7% under LUA (respectively, 1.13% under LUB) leads to an increase of 3.6% (respectively, 5.4%) in 10-year flood by considering WaSiM. The difference in the land use maps for the different time horizons was clearly translated into the change in quantile simulated by WaSiM. As the time horizon increases, it should be expected an increase in flood quantile due to an increase in agricultural and pasture and this was successfully reproduced by WaSiM (Fig. 4b) but not by SWAT model. For WaSiM model, it was clearly observed that the highest percentage changes in the quantile were related to the lower return periods for any given scenario with a possible exponential relation between these two variables. In contract, with SWAT model, there is a mixed pattern. A boxplot of the ten behavioural solutions for each scenario, each time horizon and each model reveals high variability in the change of quantiles (Figs. 9, 10 in the Appendix).

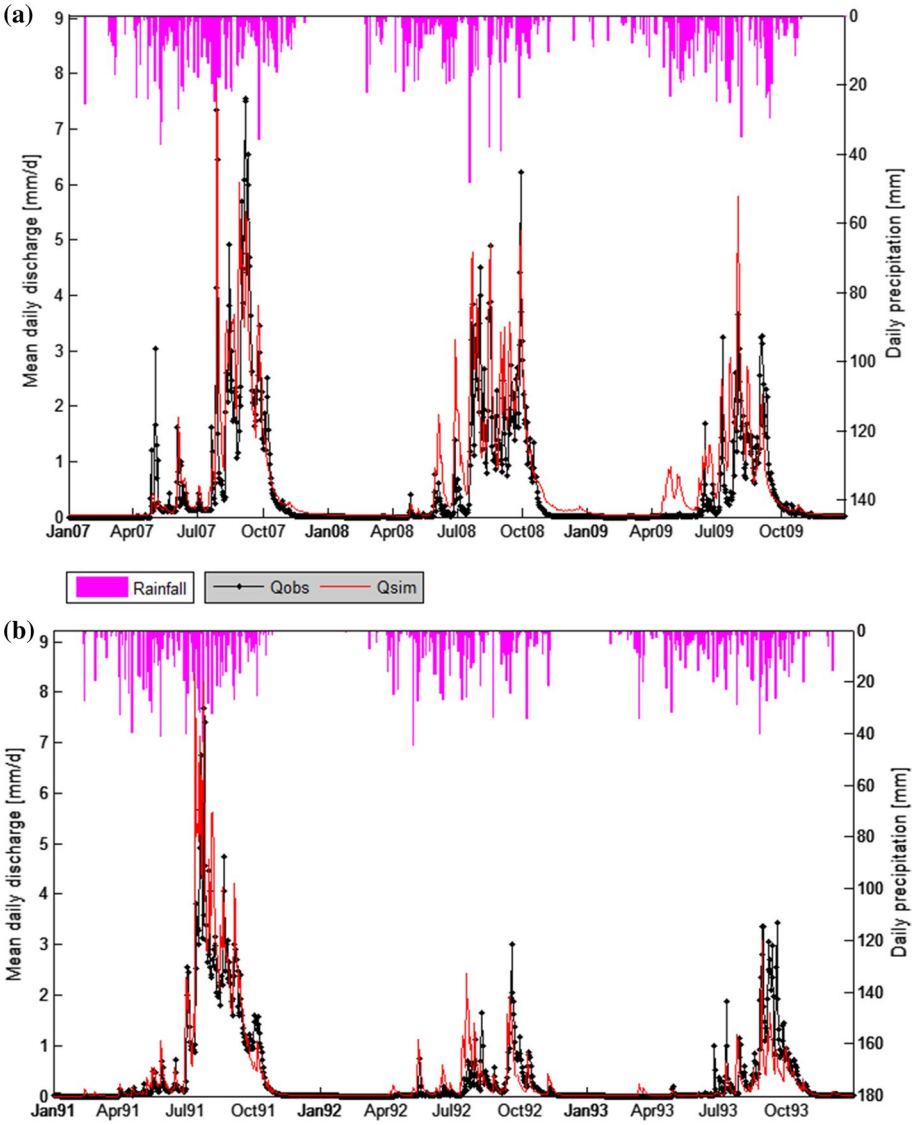

Fig. 2 Observed and simulated discharges by WaSiM (**a**) for 2007–2009 for the calibration period (using a threshold of 0 mm/d, KGE = 0.72 and APB = 11.8%; using a threshold of 1.5 mm/d, KGE = 0.6 and APB = 5%.) and by SWAT (**b**) for 1991–1993 for the validation period (using a threshold of 0 mm/d, KGE = 0.80 and APB = 5.5%; using a threshold of 1.5 mm/d, KGE = 0.39 and APB = 8.5%)

4.3.2.2 Relationship between change in land use type and change in flood quantiles Through a linear regression model between the percentage change of the different LULC types and the percentage change in quantile corresponding to the 40-year return period, we found that change in quantile could be explicated by considering change in the different land use types (Fig. 5). Indeed, strong and statistically significant relation at the level of 5% was found between these two variables with fitting statistics *p* value less

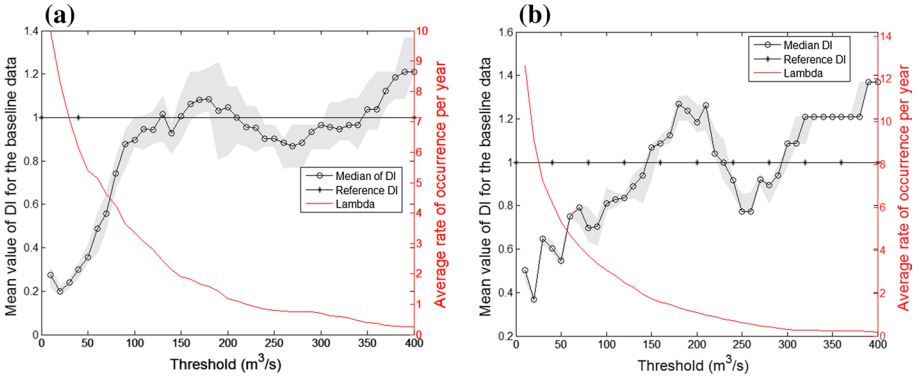

Fig. 3 Dispersion index (DI) median, the band between the 25th and the 75th percentiles of DI (in grey) and Lambda (the average rate of occurrence per year) for WaSiM (**a**) and SWAT (**b**)

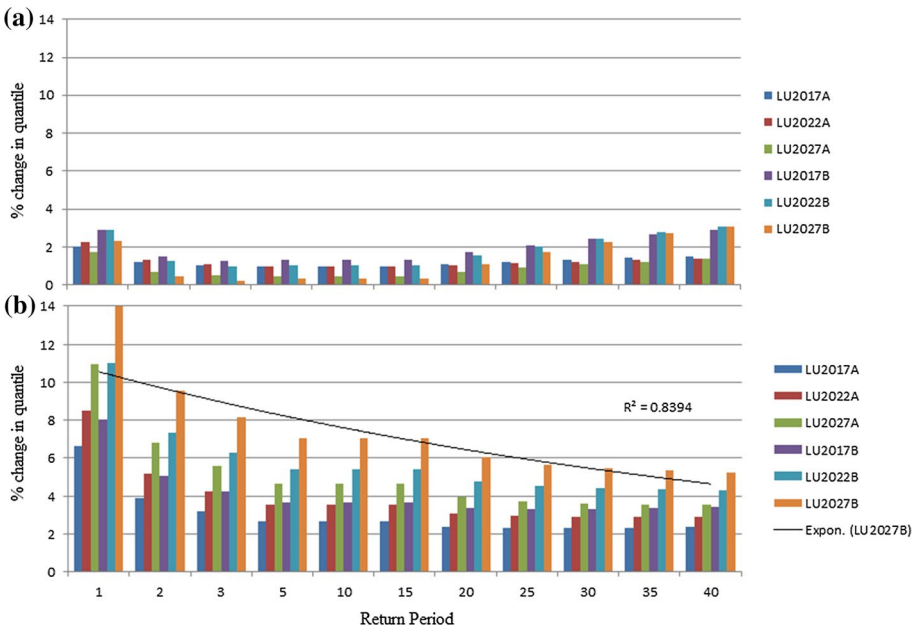

Fig. 4 Mean percentage change of flood quantiles for different land use scenarios as simulated by SWAT (**a**) and WaSiM (**b**)

than 0.05 and *R*-square varying between 0.67 and 0.99 (for all various land use types) for WaSiM (Fig. 5a–e). For SWAT, the fitting was statistically significant for three land use types at 5% and not significant for two land use types (Fig. 5f–j). Both models indicated that (Fig. 5) flood magnitude and percentage of remaining natural vegetation (forests and range brush) are negatively correlated (a, b, c, f, g, h) while flood quantile and croplands area (agriculture and pasture) are positively correlated (d, e, i, j). The decrease in natural vegetation was found to better explain the increase in flood severity than the expansion of agricultural lands (see R^2, a, b, c) for WaSiM. In contrast, with SWAT, the expansion of

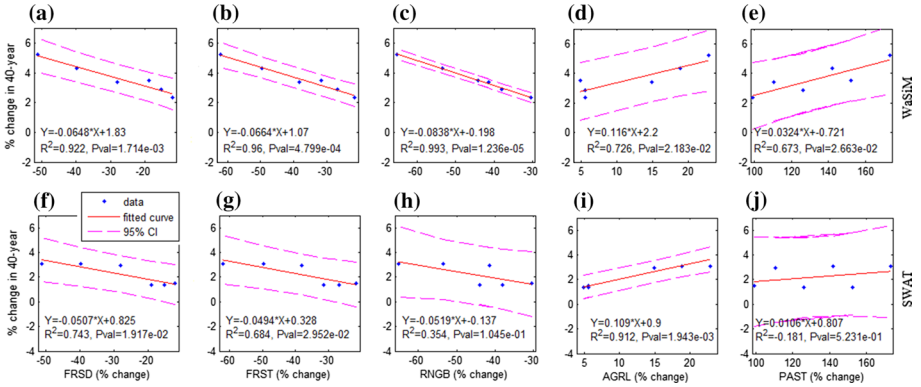

Fig. 5 Change in 40-year quantile explained by the change in different land use types by WaSiM (**a**–**e**) and SWAT (**f**–**j**). R^2 is the coefficient of determination while Pval is the p value for the F test

agricultural land explains better the increase in flood magnitude than the decrease in natural vegetation (i). These findings highlight the growing challenges for water resources managers and planners and emphasize the need to address land use changes impact on water resources while developing water management plans. Additionally, hard options such as reinforcing the riverbanks, dredging rivers and raising houses as well as redirecting flood runoff through the use of floodwalls and flood gates need to be taken to reduce flood impacts on human and properties.

The land use unit showing the strongest relation with 40-year flood event was range brush (RNGB) for WaSiM and agriculture for SWAT. These land use types were used to evaluate the strength of this relation with other quantiles (Fig. 6). The obtained high value of R^2 and p value < 0.05 confirmed that change in flood magnitudes can be imputed to change in land use types. This relationship became stronger (expressed by the increasing R^2 and the decreasing 95% uncertainty bounds) as the flood magnitude increases, implying that the effects of the conversion of natural vegetation into agricultural land are more expressed on flood with high return periods. Alila et al. (2009) found similar results. They state that floods with high return periods can be more impacted compared to the flood with small or medium return periods after forest harvest. Many other authors (including La Marche and Lettenmaier 2001; Verry et al. 1983) came to the same conclusions.

This relation is stronger with WaSiM than with SWAT. The fitted linear regression models with RNGB (range brush) explain more than 94% of the variability in the change in different quantiles for WaSiM model while AGRL (agriculture) helps to explain more than 60% of the variability in the change of the quantile corresponding to return period greater than or equal to 25 years. For return period lower than 25 years, the fit obtained from SWAT output was not satisfactory with p value > 0.05 and $R^2 < 0.29$.

4.3.3 Relating change in LULC to change in return periods

Whatever the scenarios and the hydrological model are, small changes in the magnitude observed in the previous section will cause flood events to become more frequent than currently observed (Fig. 7) and the frequency is more accentuated for land use scenario B (LUB) than the land use scenario A (LUA). The average new return period under LUA was 25 (respectively, 28) and 22 under LUB (respectively, 27) for WaSiM (respectively,

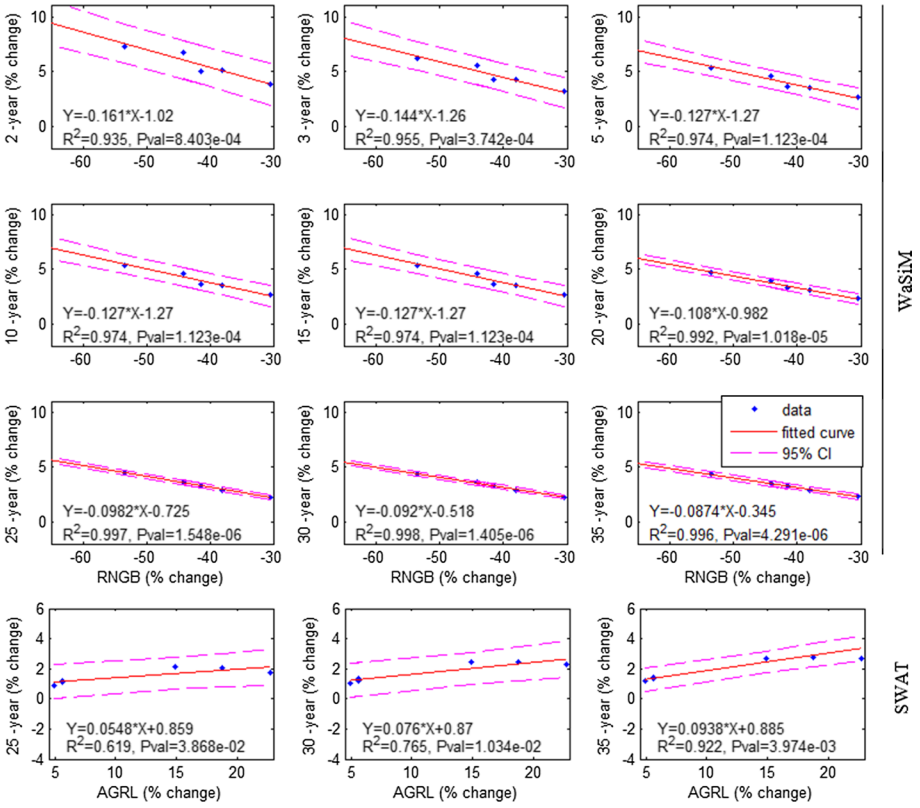

Fig. 6 Relationships between percentage change in flood quantiles and percentage change in land use types. R^2 is the coefficient of determination while Pval is the p value for the F test

SWAT) for current 30 years. Nevertheless, only WaSiM model reproduced acceptably the difference in the land use maps for the different time horizons in terms of return periods. For instance, considering a current 30-year return period and under the scenario A, the new return periods for 2017, 2022 and 2027 are, respectively, 26, 25 and 24 years for WaSiM while the same value of 28 years was computed for SWAT during these periods.

Our results have shown for the first time that the reduction in natural vegetation at the yearly rate of 0.7% under land use scenario A (respectively, 1.13% under land use scenario B) leads a current 2-year flood event to becoming 1.7 years (respectively, 1.6 years), current 10-year flood event to become 8.6 years (respectively, 7.9 years) and current 40-year flood event to become 32.6 years (respectively, 29.4 years) in average for WaSiM model. Similarly, the reduction in natural vegetation at the yearly rate of 0.7% under land use scenario A (respectively, 1.13% under land use scenario B) leads a current 2-year flood event to become 1.9 years (respectively, 1.9 years), current 10-year flood event to become 9.7 years (respectively, 9.5 years) and current 40-year flood event to become 37.4 years (respectively, 34.8 years) in average for SWAT.

As it was done for flood quantile, a linear regression model was fitted to the corresponding new return periods (under the land use changes scenarios) for a current 40-year flood and the percentage change of each land use type (Fig. 8). The goodness-of-fit measures

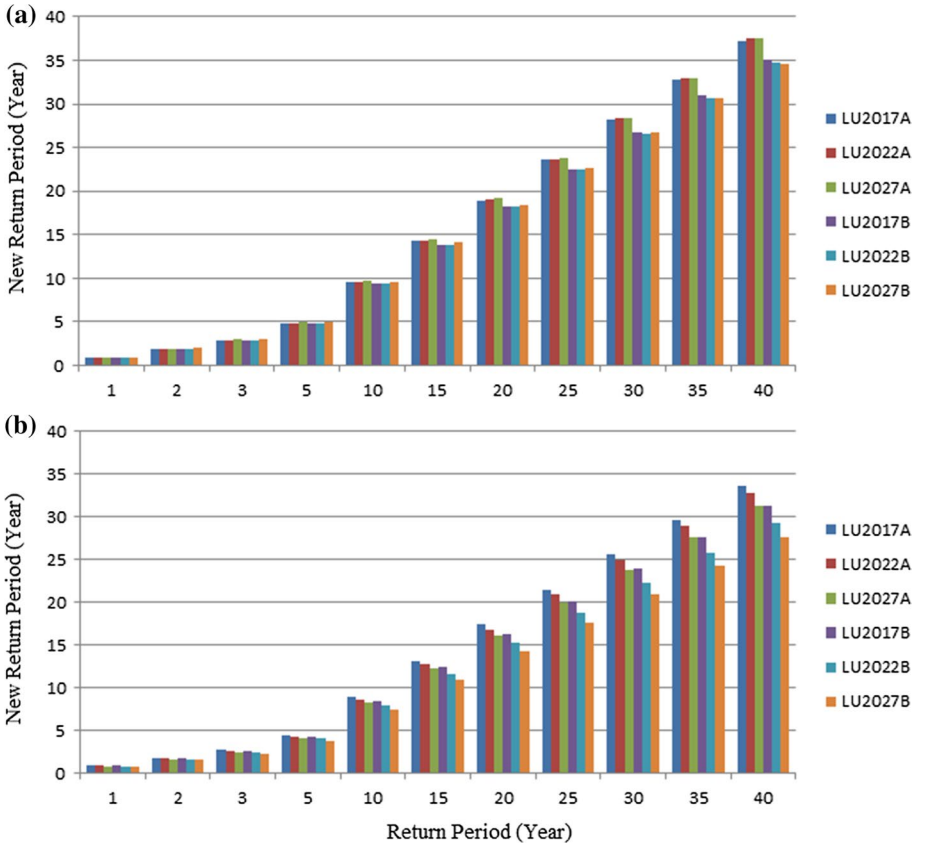

Fig. 7 Corresponding new return periods after applying the different scenarios using SWAT (**a**) and WaSiM (**b**)

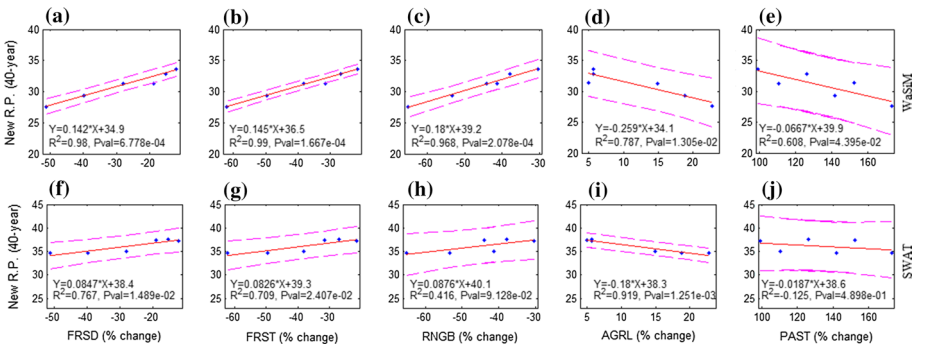

Fig. 8 Relationships between floods return periods and percentage change of each land use type as simulated by WaSiM (**a**–**e**) and SWAT (**f**–**j**). R^2 is the coefficient of determination while Pval is the p value for the F test

found were statistically significant at 5% level for all land use types for WaSiM but for three land use types for SWAT. Change in return periods could be attributed to a modification in land use types. The percentage change in forest (FRST) explained about 99% (71%, respectively) of the variation in the 40-year return period for WaSiM (for SWAT, respectively). In contrast, AGRL (agriculture) explained about 79% (92%) of the variability in the 40-year RP according to WaSiM (SWAT). WaSiM reproduced very well the decrease in natural vegetation in comparison with SWAT model. In contrast, the increase in agricultural land was better reproduced by SWAT than by WaSiM.

5 Discussion

5.1 Land use and land use change scenarios

The projection of land use of a catchment is inherent to more errors than climate projection mainly because of many factors (Götzinger 2007) such as political, economic, technical and natural boundary conditions. Nevertheless, this estimation is necessary for evaluating future changes in LULC for impact studies. The two LULC scenarios were essentially based on population growth (3.1% for land use scenario A and 3.5% for land use scenario B) and consequent transformation of different types of forests into agricultural lands and pasture. Three time slices were considered for each scenario: 2015–2019, 2020–2024 and 2025–2029. With the uncertainties inherent to any land use projection, an increase in croplands and pasture at annual rate of 0.7% under land use scenario A and 1.13% under land use scenario B were found between 2003 and 2029. This rate was small compared to 3% found by Orekan (2007) between 1995 and 2006 in Benin. The decrease in natural formation due to population growth was observed by Yira et al. (2016) in West Africa.

5.2 Hydrological modelling

With regard to the uncertainties inherent to any hydrological modelling and more in data scarce region like West Africa, the performance of the models was unsatisfactory to good at threshold of 120 m^3/s (Table 5) but satisfactory to very good for lower thresholds implying a good agreement among observed and measured discharges. The poor quality of SWAT was due to the fact that most of the simulations that were satisfactory or better did not exhibit a good water balance components and were thus excluded. Substantial differences in the performances of models were observed as it was observed for similar studies (Huisman et al. 2009; Cornelissen et al. 2013). Based on the KGE, WaSiM was the best model compared to SWAT during both calibration and validation. Based on the average value of APB, WaSiM performances exceed SWAT records during calibration but during validation SWAT model performed better than WaSiM (Table 5).

To reduce the uncertainties of the parameters, multi-parameter ensemble approaches with a variation in model inputs have been used as recommended by many authors in the literature (Vrugt et al. 2003; McEnery et al. 2005). The uncertainties related to model are due to the simplifications inherent to model structure, and these can be reduced through the reduction in bias in model prediction by computing changes relatively to the baseline simulation (not the baseline observation data) as commonly done in scenario projections (Huisman et al. 2009; IPCC 2001). However, our confidence in model predictions is likely to increase as the model structural error is considerably reduced (Huisman et al. 2009).

Some of the limitations of the multi-modelling approach are: (a) time consumption: obviously, the time used for calibrating and validating models and the materials needed increase as the number of models increase; (b) scale issues: spatially distributed (based on grid cell for WaSiM) versus spatially semi-distributed (based on HRU which may combine many gird cells) make a significant difference in the models; (c) different equations may be used for the same hydrological process depending on the model. For instance, the direct flow is computed based on the infiltration and saturation excess approach in WaSiM while the SCS curve number is used in SWAT and (d) criteria for model inter-comparison and the choice of the best model.

5.3 LULC change impact on flood characteristics

Quantifying the influence of change in LULC (resulting from human activities) on flood severity and occurrence is relevant information for flood risk management. By combining spatially and temporally distributed land use scenarios, distributed and semi-distributed hydrological models and statistical analysis, this work has demonstrated that change in LULC significantly affects the magnitude and frequency of floods. As found by many authors in the literature (see Table 1), an increase in flood characteristics was observed following the expansion of agricultural lands and a decrease in natural vegetation such as the different types of forests. This increase in flood characteristics can be due to the fact that crops in general consume less water in comparison with natural vegetation and agricultural land generates more surface runoff (Götzinger 2007). The expansion of croplands leads to soil consolidation and a decreased in hydraulic conductivity. This implies a reduction in soil infiltration capacity and therefore a production of more surface runoff (Costa et al. 2003). On the other hand, soil disturbance (Rice 1981; Guillemette et al. 2005) and change in vegetation characteristics through the rainfall interception and evapotranspiration capacities (Vertessy et al. 2002; Farley et al. 2005) can explain the increasing flood risk. Similar conclusions were drawn by many authors including Yira et al. (2016) in the Dano catchment and Mahé et al. (2005) in Nakambe catchment, both in Burkina Faso.

The same direction of change derived from the two models' outputs increases our confidence in the results. Nevertheless, the rates of change differ between models (Fig. 4). For instance, the average rate of increase in the magnitude of 2-year flood event varies between 4 and 9.6% for WaSiM model but between 0.4 and 1.5% for SWAT model. The difference in model predictions is more highlighted by considering the ensemble members of each model (Figs. 9, 10 in the Appendix) with a considerable range of variation. This difference in model outputs can be imputed to the difference in model structures. In fact, during the implementation of LULC scenarios, dominant land use types were considered in each HRU for SWAT model while for WaSiM, the real land use type was considered for each grid cell. In addition, a change in land use distribution implies a new distribution of HRUs in SWAT. The change in SWAT outputs after the scenarios implementation may not only be caused by the change in land use distribution but also by the change in hydrological response units' distribution in SWAT. Nevertheless, the variation induced by the change in HRUs is negligible compared to the change induced by the variation in land use distribution. The benefits of using an ensemble of models (Huisman et al. 2009) with different structures are to examine model outputs from scenarios with more confidence.

In the literature, most of the studies reported an increase in discharge and peak discharge due to agricultural land expansion or others without establishing a statistical relation between them (see Table 1). This study is among the first of its kind to establish

a very strong linear relation between flood characteristics and change in each land use type (Figs. 5, 6, 8). Both models are consistent about the direction of the linear relation, but substantial differences between models exist about the strength of the fitting. The 95 per cent confidence interval brackets all the data strengthening our confidence in this linear relation (Figs. 5, 6, 8). The smallest uncertainty bounds were obtained for range brush (RNGB) for WaSiM (fitting $R^2 = 0.99$) and agriculture for SWAT ($R^2 = 0.91$) (Fig. 5) by considering change in 40-year flood. A decrease in forests and range brush increases 40-year flood magnitude at a rate between 0.06 and 0.08% (Fig. 5). Based on this linear relation, a total natural vegetation cutting will turn a current 40-year flood into 21-year flood. Despite the low quality measure of SWAT during both calibration and validation, it explains better the direct relation between agriculture and change in return period and change in quantile (Figs. 5, 8) than WaSiM model.

6 Conclusion

This work aims at applying multi-modelling approach and statistical methods for evaluating possible changes in flood frequency and magnitude using LULC change scenarios. Despite the considerable range of prediction for the scenarios produced by the model ensemble, we found generally a concordance about the direction of change in the average flood frequency and severity. Compared to previous studies on LULC change scenarios using only one model, the convergence of model results strengthens our assurance in the scenario predictions. All models predicted an increase in flood frequency and severity for both scenarios. Flood risk will be even amplified if the rate of natural vegetation conversion to croplands and pastures increases to population growth rate of 3.5% as it was found in other basins. However, these results should be interpreted considering the uncertainty related to hydrological modelling, land use mapping and climate factors. An important assumption made in this study was that land use scenarios provided for future time periods do not consider climate change. Indeed, these results should not be considered as prediction, but rather what would occur under present conditions if the land use were to change. Future studies based on the combination of climate and land use changes on flood are required to get more precise projection of future change in flood characteristics.

The results of this study can be extended to other regions to get a good understanding of the direct relationship between flood severity/frequency and the dynamics of land use. This knowledge is a proxy for assessing change in sediments and nutrients transportation to the river network, availability of water resources for crops and domestic use and for developing adaptation measures for flood risk reduction. The study is interesting and useful for the research community as well as the decision makers for framing appropriate policy decisions towards the management of extreme events in future.

Acknowledgements This work was supported by the German Ministry of Education and Research (BMBF) through the West African Science Service Center on Climate Change and Adapted Land Use (WASCAL; www.wascal.org).

Appendix

See Table 7 and Figs. 9 and 10.

Table 7 Calibrated parameters of WaSiM and SWAT models and their ranges

Parameters	Meaning of the parameters	Initial ranges		Final ranges	
WaSiM model					
DD	Drainage density	1	500	139.33	249.32
KI	Interflow coefficient	1	500	35.46	89.20
Dr	Direct runoff storage coefficient	1	500	29.28	68.99
KK	Baseflow coefficient in the equation $qb = Q_{01} * \exp(-KK/z)$ (m)	0.05	2	0.60	1.18
Q_{01}	Baseflow coefficient in the equation $qb = Q_{01} * \exp(-KK/z)$ (mm d^{-1})	0.05	2	0.57	1.49
Ksat	Saturated hydraulic conductivity[1] (m s^{-1})	10E − 9	0.01	10E − 07	8.96E − 03
Krec	Recession constant with soil depth[2] (m s^{-1})	0	2	6.44E − 04	1.99
RSC	Soil surface resistance[2] (s m^{-1})	1	200	40.80	99.84
RSE	Leaf surface resistance[2] (s m^{-1})	1	200	80.48	99.78

Parameters	Type[3]	Meaning of the parameters	Initial ranges		Final ranges	
SWAT model						
SOL_AWC().sol	R	Available water capacity of the soil layer	− 1	+ 1	0.375	0.441
SURLAG.bsn	V	Surface runoff lag time	0.05	24	0.166	0.191
CH_K2.rte	V	Effective hydraulic conductivity in main channel alluvium	0	1.5	0.830	0.960
ESCO.bsn	V	Soil evaporation compensation factor	0	1	0.023	0.027
ESCO.hru	V	Soil evaporation compensation factor	0	1	0.012	0.014
CN2.mgt	A	SCS runoff curve number for moisture condition II	− 10	+ 10	− 7.762	− 6.545
RCHRG_DP.gw	V	Deep aquifer percolation fraction	0	1	0.057	0.069
ALPHA_BF.gw	V	Baseflow alpha factor (days)	0	1	0.265	0.296
GWQMN.gw	V	Treshold depth of water in the shallow aquifer required for return flow to occur (mm)	0	200	86.084	106.762
GW_SPYLD.gw	V	Specific yield of the shallow aquifer (m^3/m^3)	0	4	0.004	0.005
OV_N.hru	V	Manning's "n" value for overland flow	0.01	30	0.236	0.281
EPCO.hru	V	Plant uptake compensation factor	0	1	0.912	0.987
GW_DELAY.gw	V	Groundwater delay (days)	0	100	31.330	35.499
REVAPMN.gw	V	Threshold depth of water in the shallow aquifer for "revap" to occur (mm)	0	50	0.017	0.020
GW_REVAP.gw	V	Groundwater "revap" coefficient	0	0.2	0.195	0.198
SOL_K().sol	R	Saturated hydraulic conductivity	− 1	+ 1	− 0.869	− 0.806
SOL_BD().sol	R	Moist bulk density	− 1	+ 1	0.175	0.209

(1) for each soil type and soil layer; (2) for each land use type and (3)—**V** means the existing parameter value is to be replaced by the given value, **A** means the given value is added to the existing parameter value, and **R** means the existing parameter value is multiplied by (1 + a given value)

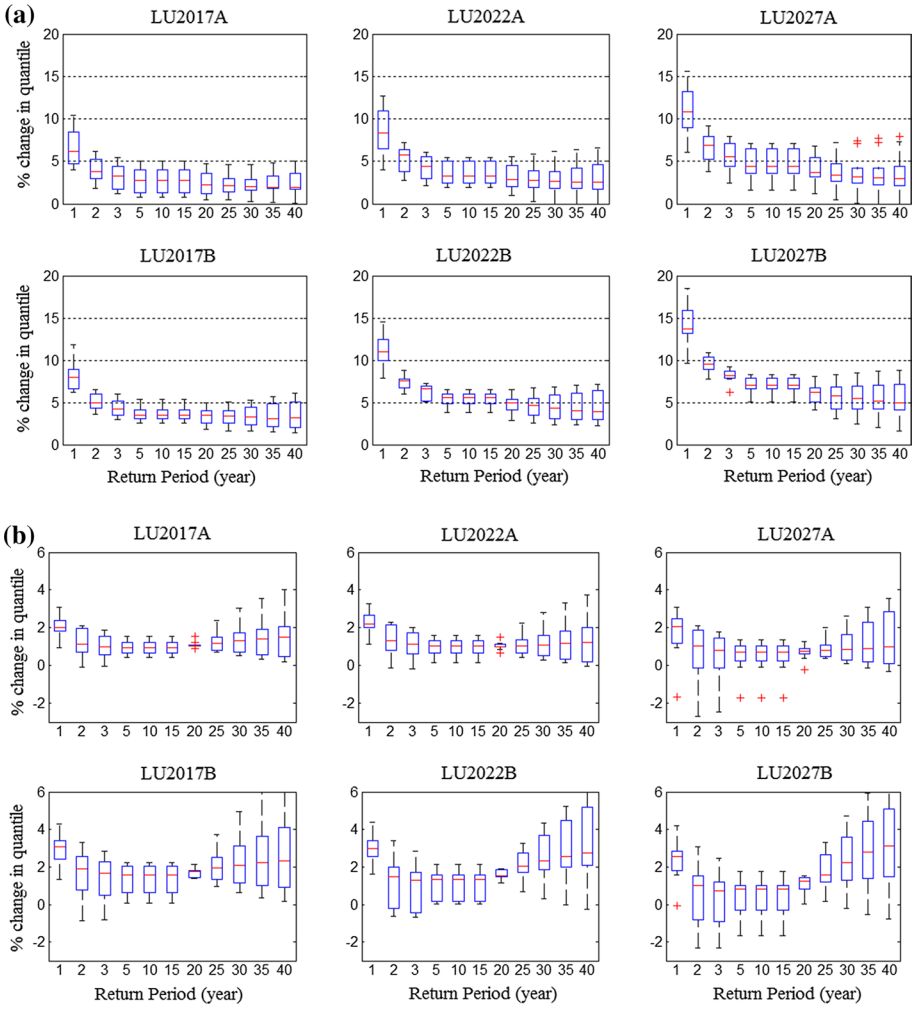

Fig. 9 Percentage changes in *x*-year quantile and the corresponding new return periods as computed from WaSiM for the different scenarios. Three time windows have been chosen for the two land use scenarios: 2015–2019 (LU2017A, LU2017B); 2020–2024 (LU2022A, LU2022B); and 2025–2029 (LU2027A, LU2027B)

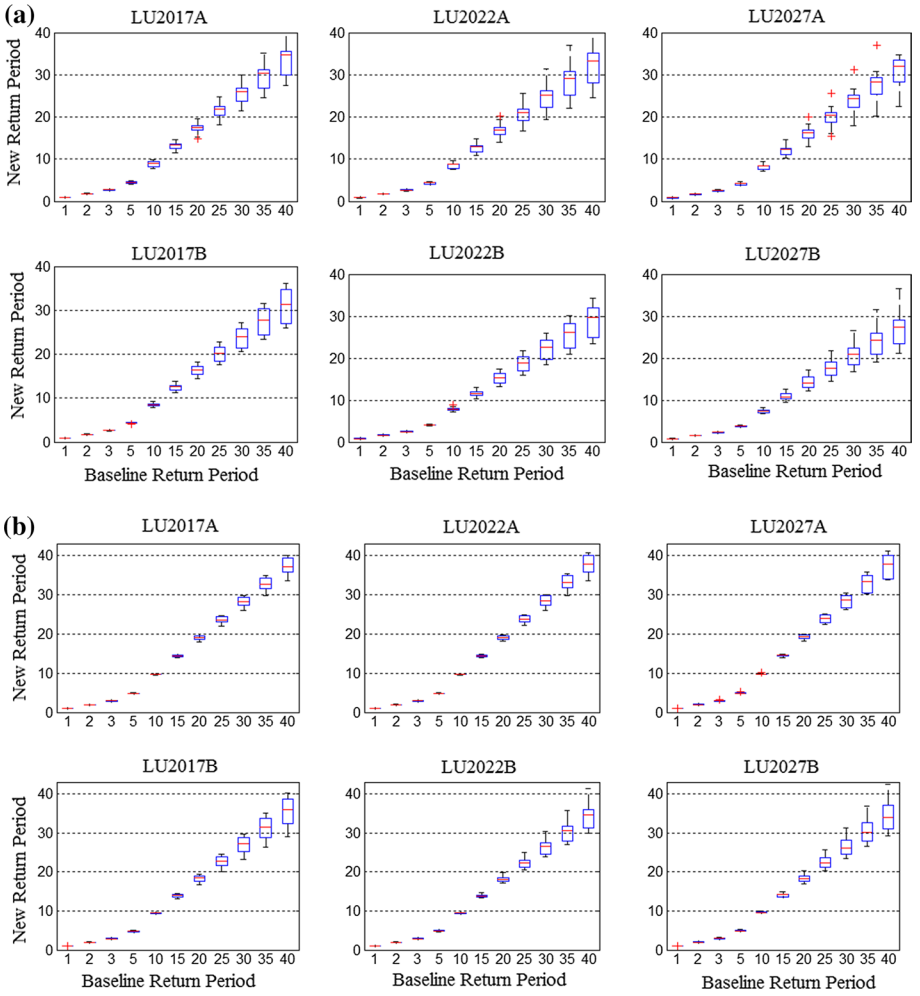

Fig. 10 Percentage changes in *x*-year quantile and the corresponding new return periods as computed from SWAT for the different scenarios. Three time windows have been chosen for each land use scenario: 2015–2019 (LU2017A, LU2017B); 2020–2024 (LU2022A, LU2022B); and 2025–2029 (LU2027A, LU2027B)

References

Alila Y, Kura PK, Schnorbus M, Hudson R (2009) Forests and floods: a new paradigm sheds light on age-old controversies. Water Resour Res 45:1–24. https://doi.org/10.1029/2008WR007207

Arnell NW (1999) The effect of climate change on hydrological regimes in Europe: a continental perspective. Glob Environ Change 9:5–23

Arnold JG, Srinivasan R, Muttiah RS, Williams JR (1998) Large area hydrologic modeling and assessment part I: model development. J Am Water Resour As 34:73–89

Beguería S (2005) Uncertainties in partial duration series modelling of extremes related to the choice of the threshold value. J Hydrol 303:215–230. https://doi.org/10.1016/j.jhydrol.2004.07.015

Beven K (2012) Rainfall-runoff modelling, the primer, 2nd edn. Wiley, Oxford, p 472

Beven K, Freer J (2001) Equifinality, data assimilation, and uncertainty estimation in mechanistic modelling of complex environmental systems using the GLUE methodology. J Hydrol 249:11–29. https://doi.org/10.1016/S0022-1694(01)00421-8

Bormann H, Breuer L, Gra T (2009) Assessing the impact of land use change on hydrology by ensemble modelling: IV. Model sensitivity to data aggregation and spatial (re-) distribution. Adv Water Resour 32:171–192. https://doi.org/10.1016/j.advwatres.2008.01.002

Bossa YA (2012) Multi-scale modeling of sediment and nutrient flow dynamics in the Ouémé catchment (Benin)–towards an assessment of global change effects on soil degradation and water quality. PhD thesis. University of Bonn

Bossa A, Diekkrüger B, Agbossou E (2014) Scenario-based impacts of land use and climate change on land and water degradation from the meso to regional scale. Water 6:3152–3181. https://doi.org/10.3390/w6103152

Bronstert A, Niehoff D, Gerd B (2002) Effects of climate and land-use change on storm runoff generation: present knowledge and modelling capabilities. Hydrol Process 529:509–529. https://doi.org/10.1002/hyp.326

Chow VT, Maidment DR, Mays LW (1988) Applied hydrology. McGraw-Hill, New York, p 570

Cornelissen T, Diekkrüger B, Giertz S (2013) A comparison of hydrological models for assessing the impact of land use and climate change on discharge in a tropical catchment. J Hydrol. https://doi.org/10.1016/j.jhydrol.2013.06.016

Costa MH, Botta A, Cardille JA (2003) Effects of large-scale changes in land cover on the discharge of the Tocantins River, Southeastern Amazonia. J Hydrol 283:206–217. https://doi.org/10.1016/S0022-1694(03)00267-1

Crochet P (2012) Flood-duration-frequency modeling application to ten catchments in Northern Iceland. Report. http://www.vedur.is/media/2012_006.pdf. Accessed 10 Nov 2016

Crooks S, Davies H (2001) Assessment of land use change in the Thames catchment and its effect on the flood regime of the river. Phys Chem Earth Part B Hydrol Ocean Atmos 26:583–591. https://doi.org/10.1016/S1464-1909(01)00053-3

Cullmann J, Mishra V, Peters R (2006) Flow analysis with WaSiM-ETH—model parameter sensitivity at different scales. Adv Geosci 9:73–77

D'Orgeval T (2006) Impact du changement climatique sur le cycle de l'eau en Afrique de l'Ouest: Modélisation et incertitudes, Ph.D. thesis. Universite Paris 6

De Roo A, Odijk M, Schmuck G et al (2001) Assessing the effects of land use changes on floods in the Meuse and Oder catchment. Phys Chem Earth 26:593–599

De Roo A, Schmuck G, Perdigao V, Thielen J (2003) The influence of historic land use changes and future planned land use scenarios on floods in the Oder catchment. Phys Chem Earth 28:1291–1300. https://doi.org/10.1016/j.pce.2003.09.005

Diekkrüger B, Söndgerath D, Kersebaum KC, McVoy CW (1995) Validity of agroecosystem models. A comparison of results of different models applied to the same data set. Ecol Modell 81:3–29. https://doi.org/10.1016/0304-3800(94)00157-D

Farley KA, Jobbagy EG, Jackson RB (2005) Effects of afforestation on water yield: a global synthesis with implications for policy. Glob Change Biol 11:1565–1576. https://doi.org/10.1111/j.1365-2486.2005.01011.x

Götzinger J (2007) Distributed conceptual hydrological modelling—simulation of climate, land use change impact and uncertainty analysis, Ph.D. thesis. University of Stuttgart

Guillemette F, Plamondon AP, Prévost M, Lévesque D (2005) Rainfall generated stormflow response to clearcutting a boreal forest: peak flow comparison with 50 world-wide basin studies. J Hydrol 302:137–153. https://doi.org/10.1016/j.jhydrol.2004.06.043

Guo H, Hu Q, Jiang T (2008) Annual and seasonal streamflow responses to climate and land-cover changes in the Poyang Lake basin. J Hydrol 355:106–122. https://doi.org/10.1016/j.jhydrol.2008.03.020

Gupta HV, Kling H, Yilmaz KK, Martinez GF (2009) Decomposition of the mean squared error and NSE performance criteria: implications for improving hydrological modelling. J Hydrol 377:80–91. https://doi.org/10.1016/j.jhydrol.2009.08.003

Herbst M, Casper MC, Grundmann J, Buchholz O (2009) Comparative analysis of model behaviour for flood prediction purposes using Self-Organizing Maps. Nat Hazards Earth Syst Sci 9:373–392. https://doi.org/10.5194/nhess-9-373-2009

Hounkpè J (2016) Assessing the climate and land use changes impact on flood hazard in Ouémé River Basin, Benin (West Africa), Ph.D. thesis. University of Abomey Calavi

Huisman JA, Breuer L, Bormann H et al (2009) Assessing the impact of land use change on hydrology by ensemble modeling (LUCHEM) III: scenario analysis. Adv Water Resour 32:159–170. https://doi.org/10.1016/j.advwatres.2008.06.009

Igué AM, Houndagba CJ, Gaiser T, Stahr K (2006) Land use/cover map and its accuracy in the Oueme Basin of Benin (West Africa). In: Conference on international agricultural research for development land. University of Bonn, Bonn, Germany, p 1:4

IPCC (2001) Climate change, 2001: the scientific basis. Contribution of Working Group I to the Third Assessment Report of the Intergovernmental Panel on Climate Change. Cambridge University Press, Cambridge, p 881

Jarvis A, Reuter HI, Nelson A, Guevara E (2008) Hole-filled seamless SRTM data V4. International Centre for Tropical Agriculture (CIAT). www.cgiar-csi.org/data/srtm-90m-digital-elevation-database-v4-1. Accessed 4 May 2013

Jasper K, Gurtz J, Lang H (2002) Advanced flood forecasting in Alpine watersheds by coupling meteorological observations and forecasts with a distributed hydrological model. J Hydrol 267:40–52. https://doi.org/10.1016/S0022-1694(02)00138-5

Jothityangkoon C, Hirunteeyakul C, Boonrawd K, Sivapalan M (2013) Assessing the impact of climate and land use changes on extreme floods in a large tropical catchment. J Hydrol 490:88–105. https://doi.org/10.1016/j.jhydrol.2013.03.036

Kasei RA (2009) Modelling impacts of climate change on water resources in the Volta Basin, West Africa, Ph.D. thesis. University of Bonn

Kharel G, Zheng H, Kirilenko A (2016) Can land-use change mitigate long-term flood risks in the Prairie Pothole Region? The case of Devils Lake, North Dakota, USA. Reg Environ Change 16:1–14. https://doi.org/10.1007/s10113-016-0970-y

Kunstmann H, Marx A, Werhahn J, Smiatek G (2006) Early flood warning for alpine catchments through coupled precipitation/river runoff—forecasts. http://www.univie.ac.at/IMG-Wien/meetings/map_d-phase/abstracts/20-floodwarn-marx.pdf. Accessed 4 May 2015

La Marche JL, Lettenmaier DP (2001) Effects of forest roads on flood flows in the Deschutes River, Washington. Earth Surf Process Landforms 26:115–134. https://doi.org/10.1002/1096-9837(200102)26:22005115:AID-ESP166%3e3.0.CO;2-O

Li Z, Liu W, Zhang X, Zheng F (2009) Impacts of land use change and climate variability on hydrology in an agricultural catchment on the Loess Plateau of China. J Hydrol 377:35–42. https://doi.org/10.1016/j.jhydrol.2009.08.007

Mahé G, Paturel J, Servat E et al (2005) The impact of land use change on soil water holding capacity and river flow modelling in the Nakambe River, Burkina-Faso. J Hydrol 300:33–43. https://doi.org/10.1016/j.jhydrol.2004.04.028

McEnery J, Ingram J, Duan Q et al (2005) NOAA's advanced hydrologic prediction service: building pathways for better science in water forecasting. Bull Am Meteorol Soc 86:375–385. https://doi.org/10.1175/BAMS-86-3-375

McKay MD, Beckman RJ, Conover WJ (2000) A comparison of three methods for selecting values of input variables in the analysis of output from a computer code. Technometrics 42:55–61

Mendizabal M, Sepulveda J, Torp P (2014) Climate change impacts on flood events and its consequences on human in Deba River. Int J Environ Res 8:221–230

Menz G, Judex M, Orékan V et al (2010) Land use and land cover modeling in Central Benin. In: Speth P, Christoph M, Diekkrüger B (eds) Impacts of global change on the hydrological cycle in West and Northwest Africa. Springer, Berlin, pp 512–535

Moriasi DN, Arnold JG, Van Liew MW et al (2007) Model evaluation guidelines for systematic quantification of accuracy in watershed simulations. Am Soc Agric Biol Eng 50:885–900

Orekan V (2007) Implementation of the local land-use and land-cover change model CLUE-s for Central Benin by using socio-economic and remote sensing data, Ph.D. thesis. http://hss.ulb.uni-bonn.de/2007/1084/1084.htm. Accessed 3 May 2015

Refsgaard JC, Knudsen J (1996) Operational validation and intercomparison of different types of hydrological models. Water Resour Res 32:2189–2202. https://doi.org/10.1029/96WR00896

Rice R (1981) A perspective on the cumulative effects of logging on streamflow and sedimentation. In: Cumulative effects of forest management on Californian watersheds. US Department of Agriculture, Forest Service Pacific Southwest Forest and Range Experiment Station, pp 36–46

Richards LA (1931) Capillary conduction of liquids through porous mediums. Physics (College Park Md) 1:318–333

RIVERTWIN (2007) Regional model for integrated water management in Twinned River Basins. Adapted and integrated model for the Ouémé River Basin, Institute for Landscape Planning and Ecology: Stuttgart, Germany, Final Report. http://cordis.europa.eu/publication/rcn/11810_de.html. Accessed 3 Jun 2015

Rohstoffe G, Hannover D (1993) Bewertung von Pedotransferfunktionen zur Schatzung der Wasserspannungskurve. Zeitschrift für Pflanzenernährung und Bodenkunde 455:447–455

Schulla J (2012) Model description WaSiM. Zürich, Switzerland. www.wasim.ch. Accessed 3 Feb 2016

Seidou O, Ramsay A, Nistor I (2012a) Climate change impacts on extreme floods II: improving flood future peaks simulation using non-stationary frequency analysis. Nat Hazards 60:715–726. https://doi.org/10.1007/s11069-011-0047-7

Seidou O, Ramsay A, Nistor I (2012b) Climate change impacts on extreme floods I: combining imperfect deterministic simulations and non-stationary frequency analysis. Nat Hazards 61:647–659. https://doi.org/10.1007/s11069-011-0052-x

Sintondji LOC (2005) Modelling the rainfall-runoff process in the Upper Ouémé catchment (Terou in Bénin Republic) in a context of global change : extrapolation from the local to the regional scale, Ph.D. thesis. University of Bonn

Teng J, Chiew FHS, Timbal B et al (2012) Assessment of an analogue downscaling method for modelling climate change impacts on runoff. J Hydrol 472–473:111–125. https://doi.org/10.1016/j.jhydrol.2012.09.024

Thanapakpawin P, Richey J, Thomas D et al (2006) Effects of landuse change on the hydrologic regime of the Mae Chaem river basin, NW Thailand. J Hydrol 334:215–230. https://doi.org/10.1016/j.jhydrol.2006.10.012

Vaze J, Teng J (2011) Future climate and runoff projections across New South Wales, Australia: results and practical applications. Hydrol Process 25:18–35. https://doi.org/10.1002/hyp.7812

Verry ES, Lewis JR, Brooks KN (1983) Aspen clearcutting increases snowmelt and storm flow peaks in north central Minnesota. Water Resour Bull 19:59–67

Vertessy Ra, Zhang L, Dawes WR (2002) Plantations, river flows and river salinity. Prospect Aust For Plant 2002(66):55–61. https://doi.org/10.1080/00049158.2003.10674890

Viney NR, Bormann H, Breuer L et al (2009) Assessing the impact of land use change on hydrology by ensemble modelling (LUCHEM) II: ensemble combinations and predictions. Adv Water Resour 32:147–158. https://doi.org/10.1016/j.advwatres.2008.05.006

Vrugt JA, Gupta HV, Bouten W, Sorooshian S (2003) A Shuffled Complex Evolution Metropolis algorithm for optimization and uncertainty assessment of hydrologic model parameters. Water Resour Res 39:1201. https://doi.org/10.1029/2002WR001642

Wagner S (2008) Water Balance in a Poorly Gauged Basin in West Africa Using Atmospheric Modelling and Remote Sensing Information. Institut für Wasserbau der, Universität Stuttgart. https://elib.uni-stuttgart.de/bitstream/11682/301/1/wagner_173_online_UB.pdf. Accessed 13 Oct 2016

Willems P (2014) WETSPRO: water engineering time series processing tool. http://www.kuleuven.be/hydr/pwtools.htm. Accessed 16 Jul 2015

Yira Y, Diekkrüger B, Steup G, Bossa aY (2016) Modeling land use change impacts on water resources in a tropical West African catchment (Dano, Burkina Faso). J Hydrol 537:187–199. https://doi.org/10.1016/j.jhydrol.2016.03.052

Affiliations

Jean Hounkpè[1,2] · Bernd Diekkrüger[3] · Abel A. Afouda[1,2] · Luc Olivier Crepin Sintondji[2]

Bernd Diekkrüger
b.diekkrueger@uni-bonn.de

Abel A. Afouda
aafouda@yahoo.fr

Luc Olivier Crepin Sintondji
o_sintondji@yahoo.fr

[1] West Africa Science Service Centre on Climate Change and Adapted Land Use, University of Abomey-Calavi, 2008 Abomey-Calavi, Benin

[2] National Water Institute, University of Abomey-Calavi, 2008 Abomey-Calavi, Benin

[3] Department of Geography, University of Bonn, Meckenheimer Allee 166, 53115 Bonn, Germany